



## Triode operation of CO poisoned PEM fuel cells: Fixed and cyclic potential triode operation

M.N. Tsampas<sup>a</sup>, F.M. Sapountzi<sup>a,\*</sup>, S. Divane<sup>a</sup>, E.I. Papaioannou<sup>a</sup>, C.G. Vayenas<sup>a,b</sup>

<sup>a</sup> Department of Chemical Engineering, University of Patras, Caratheodory 1 St., GR-26504, Greece

<sup>b</sup> Academy of Athens, Panepistimiou 28 Ave., GR-10679 Athens, Greece

### ARTICLE INFO

#### Article history:

Received 8 September 2011

Received in revised form 1 March 2012

Accepted 5 March 2012

Available online 27 March 2012

#### Keywords:

PEMFC

CO poisoning

Triode fuel cell

Overpotential minimization

### ABSTRACT

An alternative approach for enhancing the Polymer Electrolyte Membrane Fuel Cell (PEMFC) performance under CO poisoning conditions was investigated by the use of the recently developed triode fuel cell design and operation. In this mode of operation a third, auxiliary, electrode is introduced in addition to the anode and cathode electrodes. It is shown that the application of electrolytic potential between the cathode and an auxiliary electrode can affect the performance of the fuel cell circuit in a controllable and reversible manner. The applied electrolytic current or potential can be fixed (steady-state) or can be cycled between chosen limits. In the present study, both triode operation modes were investigated and it was found that the time-averaged power output of the fuel cell can be increased up to three times.

© 2012 Elsevier B.V. All rights reserved.

### 1. Introduction

Triode operation is a recently developed method for enhancing the power output and thermodynamic efficiency of batteries and fuel cells [1,2]. A triode fuel cell consists of three electrodes, i.e. apart from anode and cathode, a third electrode is also introduced. Hence, in addition to the conventional fuel cell circuit, a second auxiliary circuit is formed which is run in the electrolytic mode and permits operation of the fuel cell circuit under previously inaccessible anode–cathode potential differences [1]. Thus during triode operation some power is sacrificed in the auxiliary circuit in order to enhance the overall production of electrical power.

The concept of the triode fuel cell operation was first developed and validated using a Solid Oxide Fuel Cell (SOFC) with polarizable Pt electrodes [1]. Afterwards, the triode fuel cell design was demonstrated in state-of-the-art Polymer Electrolyte Membrane Fuel Cells (PEMFCs) operated in absence of noble metals in the anode [3] and also in PEMFCs using Pt-based anodes operated under severe CO poisoning [4] and under mild CO poisoning conditions [5]. These studies have shown that the power output of the fuel cell can be very significantly increased via application of auxiliary potential or current. Furthermore, this increase,  $\Delta P_{fc}$ , was found to be comparable with or higher than the power,  $P_{aux}$ , sacrificed in the auxiliary circuit [1–5]. Recently, Cloutier and Wilkinson [6] have pioneered the use of the triode design of a PEMFC type reactor in order to improve the

electrolysis of water and liquid methanol in a non-flowing system at ambient conditions.

Fig. 1a shows schematically the triode PEMFC design. The three electrodes are all in electrolytic contact and form two electrical circuits (Fig. 1a):

- (i) the fuel cell circuit, which comprises the anode, the cathode, and a variable resistance,  $R_{ext}$ , for dissipating the electrical power,  $P_{fc}$ , produced, and
- (ii) the auxiliary circuit, which comprises the auxiliary electrode, the cathode of the fuel cell and a potentiostat–galvanostat.

When the applied auxiliary current,  $I_{aux}$ , is zero then the fuel cell operates in the conventional mode. It produces a power, denoted by  $P_{fc}^0$ , which is the product of the fuel cell potential,  $\Delta V_{fc}^0$ , and of the fuel cell current,  $I_{fc}^0$ . Both  $\Delta V_{fc}^0$  and  $I_{fc}^0$  vary as the external resistive load of the fuel cell circuit,  $R_{ext}$ , is varied.

The triode fuel cell operation consists of imposing an electrolytic current  $I_{aux} < 0$  or potential on the auxiliary system. In this way protons migrate from the fuel cell cathode to the auxiliary electrode (Fig. 1a).

Denoting by  $I_{far}$  the net Faradaic fuel-consuming current, one notes that in view of Fig. 1 and Kirchoff's first law it is:

$$I_{far} = I_{fc} + I_{aux} \quad (1)$$

where  $I_{aux} < 0$  for triode operation, and the net Faradaic current  $I_{far}$  corresponds via Faraday's Law to the net consumption of fuel at the anode or the net consumption of  $O_2$  at the cathode.

It is well known, that one of the main problems associated with the practical utilization of PEMFC units is that of CO poisoning of

\* Corresponding author. Tel.: +30 2610997860; fax: +30 2610997269.  
E-mail address: fenia@chemeng.upatras.gr (F.M. Sapountzi).

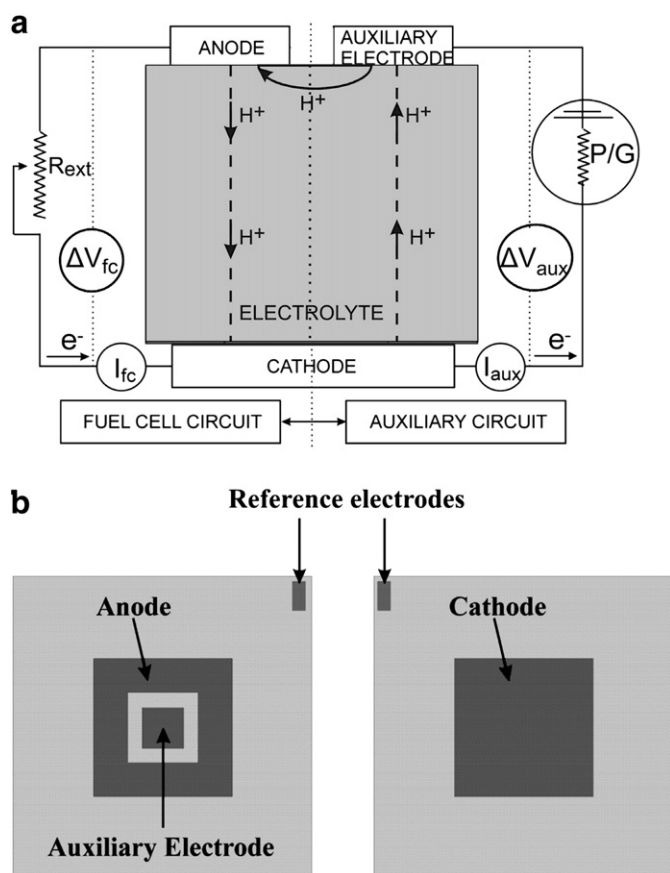


**Fig. 1.** Schematic of the triode fuel cell concept, showing the fuel cell and auxiliary circuit in detail (a) and the geometry of the membrane electrode assembly (b). The fuel cell cathode acts simultaneously as an electrode of the auxiliary circuit. P/G: potentiostat-galvanostat.

the Pt-based anode [7–9]. The aim of the present study is to study the possibility of enhancing the performance of a CO poisoned PEMFC using the triode operation, both under steady-state (fixed) and under cyclic potential application in the auxiliary circuit.

## 2. Experimental

A state-of-the-art PEMFC [3] was used (NuVant) with state-of-the-art Pt and Pt-Ru electrodes deposited by NuVant on E-TEK carbon cloth and equipped with a third auxiliary electrode.

The exact geometry of the membrane electrode assembly (MEA) used in the present investigation is shown in Fig. 1b. The MEA also includes two reference electrodes which permit direct measurement of the anodic and cathodic overpotential.

The loading of the Pt electrode was  $0.5 \text{ mg Pt/cm}^2$  (unsupported Pt black) and the loading of the Pt (30%) Ru (15%), supported on Vulcan XC-72 carbon, was  $0.5 \text{ mg/cm}^2$ . The superficial surface area of the cathode (Pt) was  $5.29 \text{ cm}^2$ , of the anode (PtRu) was  $3.85 \text{ cm}^2$  and of the auxiliary electrode (PtRu) was  $0.49 \text{ cm}^2$  (Fig. 1b). The cathode was a square and the auxiliary electrode was a smaller square located in the center of the hollow square anode (Fig. 1b). The membrane was Nafion 117 with nominal thickness of  $185 \mu\text{m}$ . The membrane electrode assembly (MEA) was prepared by hot pressing in a model C Carver hot press at  $120 \text{ }^\circ\text{C}$  and under pressure of 1 metric ton for 3 min.

Two cells were used in order to check reproducibility and both gave practically the same results. Preliminary investigation showed that the applied auxiliary potential,  $\Delta V_{\text{aux}}$ , should not exceed  $-1.9 \text{ V}$ , as this leads to  $\text{CO}_2$  formation at the cathode via oxidation of the

carbon support. The concentration of CO and  $\text{CO}_2$  in the anode and cathode feed and effluent was monitored using a Fuji Electric's Infrared Analyzer ZRJ-4UNOR 6 N IR CO/ $\text{CO}_2$  analyzer.

The gas feeds to the cathode and anode compartments (the latter includes also the auxiliary electrode, Fig. 1) were continuously humidified using thermostated gas saturators. The cell temperature was typically set at the same temperature ( $25 \text{ }^\circ\text{C}$ ) with the gas saturators. The anode compartment gas feed was Messer Griesheim certified gas mixtures of 500 ppm CO/ $\text{H}_2$ , which could be further diluted with Air Liquide (N4.5)  $\text{H}_2$ . The cathode feed was humidified by Air Liquide synthetic air.

The fuel cell circuit included a decade resistance Box (Time Electronics Ltd 1051) in order to vary the external load. The current and the potential were measured by two digital multimeters (Metex ME 21). For the fixed triode operation, constant potentials or currents in the auxiliary circuit were applied using an AMEL 553 Potentiostat-Galvanostat. For the cyclic triode operation an AMEL 567 Function Generator was used together with the Potentiostat-Galvanostat.

It is evident from Fig. 1a that all three electrodes operate in a corrosion-type mode with part of their surface used for oxidation and part of their surface used for reduction. Despite this rather intense mode of operation no performance deterioration was observed during operation for several weeks.

## 3. Results and discussion

### 3.1. Conventional fuel cell operation

Fig. 2 shows the polarization curves obtained in the conventional fuel cell mode ( $I_{\text{aux}} = 0$ ) by varying the external resistance,  $R_{\text{ext}}$ , of the decade box from zero to  $200 \Omega$ . Data were collected both under 100 kPa hydrogen supply to the anode (squares) and under CO poisoning conditions a  $\text{H}_2$  stream containing 50 ppm CO, denoted hereafter 50 ppm CO/ $\text{H}_2$  mixture (cycles). As expected, one observes that the presence of CO causes a significant decrease in power output and creates three distinct regions [9]. In the high potential-low current region ( $R_{\text{ex}} > 19 \Omega$ ) and in the low potential-high current region ( $R_{\text{ex}} < 1 \Omega$ ) stable steady-state behavior is observed, while in the intermediate region ( $1 \Omega < R_{\text{ex}} < 19 \Omega$ ) self-sustained potential and current oscillations are obtained with a period of the order of 7 to 10 s. Similar oscillatory phenomena have been reported in the literature [3,10].

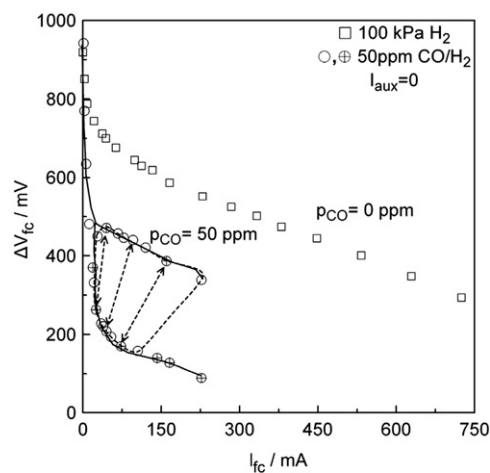


**Fig. 2.**  $I_{\text{fc}} - \Delta V_{\text{fc}}$  curves of the fuel cell circuit obtained with the conventional operation mode ( $I_{\text{aux}} = 0$ ) by varying the external resistive load,  $R_{\text{ext}}$ . Anode feed: 50 ppm CO/ $\text{H}_2$  (cycles).

Since the cell is run at constant  $R_{ext}$ , it follows that these oscillations correspond to straight line segments in the  $I-\Delta V$  plane, as shown in Fig. 2.

### 3.2. Triode operation: Fixed potential application

Fig. 3 shows a typical triode operation experiment at a constant  $R_{ext}$  equal to  $0.5 \Omega$ . A gas mixture of a  $H_2$  stream containing 50 ppm CO was supplied to the anode. Initially the fuel cell is operated in the conventional mode and the anode–cathode potential difference (cell voltage) is 140 mV while a current of 150 mA flows through the cell. Imposition of a constant electrolytic potential ( $-1.9$  V) and current ( $-21$  mA) in the auxiliary circuit causes the induction of self-sustained high amplitude oscillations in the fuel cell current (from 144 to 355 mA) and potential (from 152 to 349 mV). It is remarkable that the imposition of such a small auxiliary electrolytic current ( $I_{aux} = -15.5$  mA) causes such a pronounced increase in the current in the fuel cell circuit and in the cell voltage. The induction of this oscillatory behavior is reversible as oscillations disappear when the cell operation returns to the conventional mode ( $I_{aux} = 0$ , Fig. 3).

In order to quantify the magnitude of the enhancement two parameters have been introduced in the literature [1]: The first is the power enhancement ratio,  $\rho_P$ , defined as [1]:

$$\rho_P = P_{fc}/P_{fc}^0 \quad (2)$$

which quantifies the increase in power output in the fuel cell circuit.

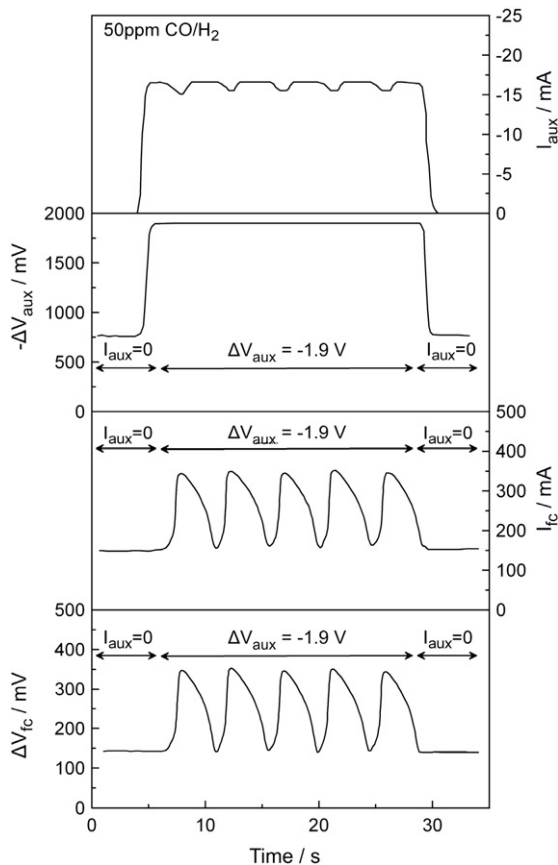


Fig. 3. Effect of a constant auxiliary potential application,  $\Delta V_{aux} = -1.9$  V on the auxiliary current  $I_{aux}$  and on the cell potential  $\Delta V_{fc}$  and cell current  $I_{fc}$ , under fixed external resistive load ( $R_{ext} = 0.5 \Omega$ ). Anode feed: Anode feed: 50 ppm CO/ $H_2$ .

The second parameter is the power gain ratio,  $\Lambda_P$ , defined as [1]:

$$\Lambda_P = (P_{fc} - P_{fc}^0) / P_{aux} \quad (3)$$

This parameter is the ratio of the increase in power output of the fuel cell circuit, divided by the power sacrificed in the auxiliary circuit,  $P_{aux}$ . The latter is the product of the auxiliary cell potential,  $\Delta V_{aux}$ , and of the auxiliary cell current,  $I_{aux}$ . When  $\Lambda_P > 1$  then the thermodynamic efficiency of the triode unit is higher than that corresponding to conventional fuel cell operation.

In the present case the time-averaged values of these two quantities are computed on the basis of Eqs. (2) and (3) from:

$$\bar{\rho}_P = \frac{1}{T} \int_0^T \rho dt \quad (4)$$

where T is the oscillation period and:

$$\bar{\Lambda}_P = \frac{\int_0^T (P_{fc} - P_{fc}^0) dt}{\int_0^T P_{aux} dt} \quad (5)$$

The power enhancement ratio,  $\rho_P$ , varies from 1 to 6, and the time-averaged enhancement  $\bar{\rho}_P$  is 3. The power gain ratio,  $\Lambda_P$ , varies from 0 to 3.4, showing that there are small time intervals where  $\Lambda_P < 1$  and thus the power gain in the fuel cell circuit is smaller than the power consumed in the auxiliary circuit. However the beneficial effect of the triode mode ( $1 < \Lambda_P < 3.4$ ) is more pronounced, thus the time-averaged power gain is approximately 1.4. Thus there is a net gain in power and thus on overall thermodynamic efficiency.

In a previous study [5] it has been confirmed by measuring the electrode potentials individually by means of two reference electrodes that this enhancement in the performance of the PEM fuel cell is mainly due to a significant decrease in anodic overpotential caused by the supply of protons to the anode via the auxiliary electrode. This proton supply increases the electrochemical potential of protons and chemical potential of hydrogen at the anode, thus, decreasing the coverage of CO and enhancing its electrooxidation rate.

### 3.3. Triode operation: Cyclic potential application

In the previous section as in previous studies [1–5] it was shown that the triode operation can be beneficial for enhancing the fuel cell performance. Previous studies [1–5] have examined constant current or constant potential imposition in the auxiliary circuit. The use of cyclic triode operation, i.e. time-varied potential application in the auxiliary circuit, is studied for the first time in this work.

Fig. 4 shows the effect of triode operation for the case of applying a time-varying electrolytic potential in the auxiliary circuit. The applied potential in the auxiliary circuit  $\Delta V_{aux}$  was varied between the values of  $-1$  V and  $-1.9$  V (in this auxiliary potential range the auxiliary current remains electrolytic), with a sweep rate of  $0.2$  V/s. Depicted in this figure is the effect of cyclic electrolytic potential application in the auxiliary circuit, on the auxiliary circuit current (top panel) and on the fuel cell current,  $I_{fc}$ , and potential (cell voltage),  $U_{fc}$  (bottom two panels) at the same fixed external resistive load ( $R_{ext} = 0.5 \Omega$ ) as in Fig. 3.

One observes that imposition of the cyclic electrolytic potential (between  $-1.0$  and  $-1.9$  V) and current (between  $-3$  and  $-18$  mA) in the auxiliary circuit causes the induction of self-sustained oscillations in the fuel cell current and in the cell voltage. The induction of this oscillatory behavior is reversible as oscillations disappear when the cell operation returns to the conventional mode ( $I_{aux} = 0$ , Fig. 4).

Fig. 5 is based on Fig. 4 and presents the time variation of the fuel cell power output,  $P_{fc}$ , the power sacrificed in the auxiliary cell,  $P_{aux}$ , of

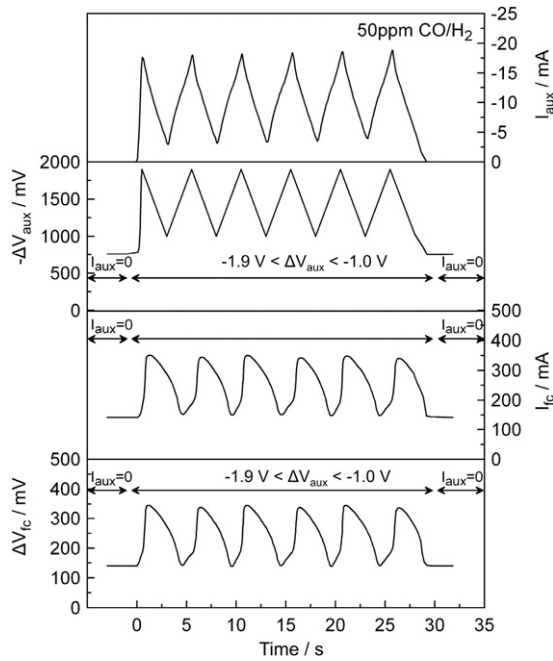


**Fig. 4.** Effect of a cyclic auxiliary potential application,  $1.0\text{ V} \leq -\Delta V_{aux} \leq 1.9\text{ V}$  on the auxiliary current  $I_{aux}$  and on the cell potential  $\Delta V_{fc}$  and cell current  $I_{fc}$ , under fixed external resistive load ( $R_{ext} = 0.5\ \Omega$ ). Anode feed: 50 ppm CO/H<sub>2</sub>.

the power enhancement ratio,  $\rho_p (= P_{fc}/P_{fc}^0)$ , and of the power gain ratio,  $\Lambda_p (= \Delta P_{fc}/P_{aux})$  and also the corresponding time-averaged values of these quantities.

The power enhancement ratio,  $\rho_p$ , varies from 1 to 5.9, and the time-averaged enhancement  $\bar{\rho}_p$  is 3. The power gain ratio,  $\Lambda_p$ , varies from 0 to 4.8, showing that there are small time intervals where  $\Lambda_p < 1$  and thus the power gain in the fuel cell circuit is smaller than the power consumed in the auxiliary circuit. However the beneficial effect of the triode mode ( $1 < \Lambda_p < 4.8$ ) is more pronounced, since the time-averaged power gain is approximately 2.3. Thus there is a net gain in power and thus on overall thermodynamic efficiency and

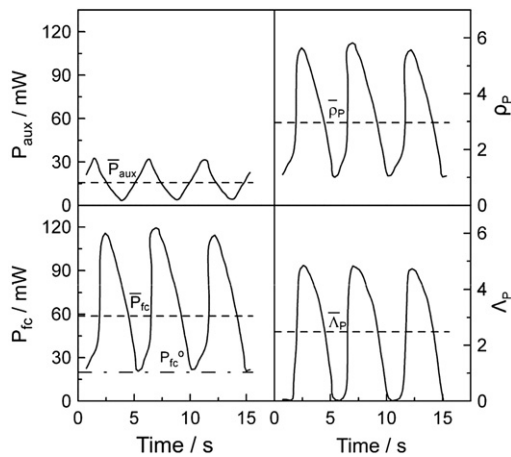


**Fig. 5.** Time variation of fuel cell power output,  $P_{fc}$ , sacrificed power in the auxiliary cell,  $P_{aux}$ , power enhancement ratio,  $\rho_p$ , and power gain ratio,  $\Lambda_p$  and corresponding time-averaged values for triode operation during imposition of a cyclic auxiliary potential,  $1.0\text{ V} \leq -\Delta V_{aux} \leq 1.9\text{ V}$ , under a fixed external resistive load ( $R_{ext} = 0.5\ \Omega$ ). Anode feed: 50 ppm CO/H<sub>2</sub>.

moreover it seems that the cyclic triode operation is more beneficial in terms of energy gain compared to the fixed triode operation.

The polarization  $I - \Delta V$  curves obtained during normal ( $I_{aux} = 0$ ) and cyclic triode operation, in all  $R_{ext}$  regions are given in Fig. 6. The region of self-sustained oscillations is extended via the cyclic triode operation and thus the time-averaged fuel cell performance is enhanced.

Since cyclic triode operation seems to be more advantageous than the fixed triode operation, it is worth of deeper investigation. A thorough examination of the effect of the period and the amplitude of the applied electrolytic potential could lead to further understanding of the exact mechanism of the triode operation.

**4. Conclusions**

The power output of a CO poisoned PEM fuel cell can be significantly enhanced via triode operation. For the first time, the effect of application of both a fixed and a time-varied potential application in the auxiliary circuit (cyclic triode operation) was investigated. It was found that under a standard applied external resistance of  $0.5\ \Omega$ , the fuel cell power output during triode operation can be three times larger than that during the conventional operation. This observed increase in the cell power output can be up to 140 and 230% larger than the power sacrificed in the auxiliary circuit, for fixed and cyclic triode operation respectively. Therefore, a net gain in power and on overall thermodynamic efficiency is evidenced for both cases. Each of the triode operation modes has its own merits and appears to be useful tool for reducing the CO poisoning effect over wide range of PEMFC operating conditions. This enhancement in power production is possible only when the working electrode is at least partly polarizable and thus the ionic conduction in the electrolyte is not rate limiting, i.e. under high Wagner number conditions [1,11]. Application of the triode operation in suitably modified PEMFC stacks for the practical application also appears feasible, using the bipolar electrolysis concept [12], as described in detail in literature [5].

**Acknowledgements**

We are thankful to the Greek Ministry of Development-GSRT “SYNERGASIA” Program (09SYN-42-729) for partial financial support.

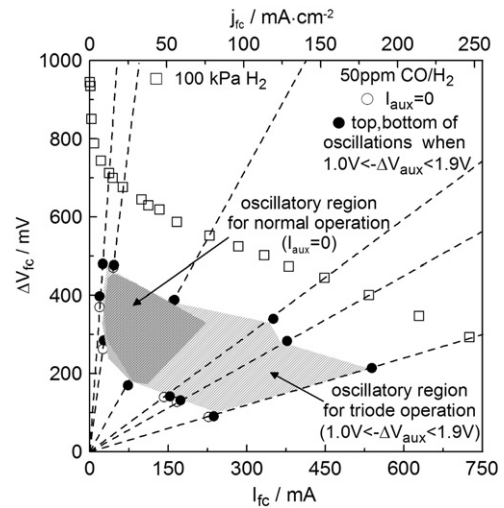


**Fig. 6.** Effect of cyclic auxiliary potential application ( $1.0\text{ V} \leq -\Delta V_{aux} \leq 1.9\text{ V}$ ) on the limits of fuel cell current-potential oscillations. The dark and light dashed areas show the region of self-sustained oscillations for normal and triode operation respectively. Anode feed: 50 ppm CO/H<sub>2</sub>.

**References**

- [1] S.P. Balomenou, C.G. Vayenas, J. Electrochem. Soc. 151 (11) (2004) A1874.
- [2] S. Balomenou, C.G. Vayenas, WO 2005/008820 (2005).
- [3] A. Katsaounis, S. Balomenou, D. Tsiplakides, S. Brosda, S. Neophytides, C.G. Vayenas, Appl. Catal. B Environ. 56 (2005) 251.
- [4] S.P. Balomenou, F. Sapountzi, D. Presvytes, M. Tsampas, C.G. Vayenas, Solid State Ionics 177 (2006) 2023.
- [5] F.M. Sapountzi, S.C. Divane, M.N. Tsampas, C.G. Vayenas, Electrochim. Acta 56 (2011) 6966.
- [6] C.R. Cloutier, D.P. Wilkinson, ECS Trans. 25 (2010) 47.
- [7] S. Ye, in: J. Zhang (Ed.), Springer-Verlag, London, 2008.
- [8] A.H. Thomason, T.R. Lalk, A.J. Appleby, J. Power. Sources 135 (2004) 204.
- [9] C.G. Farrell, C.L. Gardner, M. Ternan, J. Power. Sources 171 (2007) 282.
- [10] R. Hanke-Rauschenbach, M. Mangold, K. Sundmacher, Rev. Chem. Eng. 27 (2011) 23.
- [11] L.P.L. Carrette, K.A. Friedrich, M. Huber, U. Stimming, Phys. Chem. 3 (2001) 320.
- [12] W. Hanni, A. Perret, and Ch. Comninellis, Electrolytic cell with bipolar electrode including diamond, US Patent No. 6306270 (2001).